

Dissipation in Poynting-flux Dominated Flows: the σ -Problem of the Crab Pulsar Wind

J. G. Kirk and O. Skjæraasen

Max-Planck-Institut für Kernphysik, Postfach 103980, D-69029 Heidelberg, Germany

john.kirk@mpi-hd.mpg.de olaf.skjaeraasen@mpi-hd.mpg.de

Received ...

ABSTRACT

Flows in which energy is transported predominantly as Poynting flux are thought to occur in pulsars, gamma-ray bursts and relativistic jets from compact objects. The fluctuating component of the magnetic field in such a flow can in principle be dissipated by magnetic reconnection, and used to accelerate the flow. We investigate how rapidly this transition can take place, by implementing into a global MHD model, that uses a thermodynamic description of the plasma, explicit, physically motivated prescriptions for the dissipation rate: a lower limit on this rate is given by limiting the maximum drift speed of the current carriers to that of light, an upper limit follows from demanding that the dissipation zone expand only subsonically in the comoving frame and a further prescription is obtained by assuming that the expansion speed is limited by the growth rate of the relativistic tearing mode. In each case, solutions are presented which give the Lorentz factor of a spherical wind containing a transverse, oscillating magnetic field component as a function of radius. In the case of the Crab pulsar, we find that the Poynting flux can be dissipated before the wind reaches the inner edge of the Nebula if the pulsar emits electron positron pairs at a rate $\dot{N}_{\pm} > 10^{40} \text{ s}^{-1}$, thus providing a possible solution to the “ σ -problem”.

Subject headings: pulsars: general – pulsars: Crab – MHD – plasmas

1. Introduction

Powerful outflows in which energy is transported predominantly as Poynting flux rather than kinetic energy arise in several astrophysical contexts. These include pulsars (Gunn

& Ostriker 1969; Rees & Gunn 1974), gamma-ray bursts (Usov 1992; Spruit 1999; Lyutikov & Blackman 2001), and the jets from galactic compact objects and active galactic nuclei (Lovell et al 2002). An important generic property of such flows is that they are highly relativistic. Force-free solutions, valid in the inner regions, indicate that radial flows accelerate quickly (Buckley 1977; Contopoulos & Kazanas 2002) until they cross the fast magnetosonic point, at which their bulk Lorentz factor γ satisfies $\gamma = \sqrt{\sigma}$. The parameter σ , which is the ratio of Poynting flux to particle-born energy flux is by definition large under these conditions. Eventually, such flows release their energy into particles and/or radiation. In principle, this can happen if the flow diverges sufficiently rapidly and is thus forced to accelerate. However, this occurs only very slowly for ideal relativistic MHD flows which are initially radial (Beskin et al 1998; Chiueh, Li & Begelman 1998; Bogovalov & Tsinganos 1999; Bogovalov 2001; Lyubarsky & Eichler 2001; Lyubarsky 2002a). In the case of non-steady winds, such as those driven by an obliquely rotating magnetic dipole, the current required to support the oscillating component of the magnetic field decreases more slowly with radius than the density of available charge carriers (Usov 1975; Melatos & Melrose 1996). Consequently, the ideal MHD approximation must break down at some point in the outflow where the implied minimum drift speed reaches that of light. However, internal dissipative effects may intervene before this stage is reached, reducing the wave amplitude and decreasing the required current. Shock fronts, which provide efficient dissipation for low σ flows, are rather slow to dissipate the energy of a Poynting-flux dominated outflow, although they may be effective if the particle density is high (Lyubarsky 2002b). An alternative is dissipation by annihilation or reconnection of the oscillating part of the magnetic field (Coroniti 1990; Michel 1994), and this is the process we investigate in detail in this paper. The effectiveness of such a dissipation mechanism is an important ingredient in models of pulsed high energy radiation from pulsar winds (Kirk et al 2002; Skjæraasen et al. 2002; Skjæraasen & Kirk 2001) and the after-glows of gamma-ray bursts (Drenkhahn & Spruit 2002).

Although now invoked in models of AGN jets and gamma-ray bursts (Thompson 1994; Schopper et al 1998; Heinz & Begelman 2000; Spruit et al 2001), the original motivation for considering reconnection in Poynting-flux dominated outflows was the so-called “ σ -problem”. This term is generally used to refer to a puzzle posed by the Crab Nebula and the pulsar wind which powers it: according to estimates of the number of pairs emitted by the pulsar (Arons 1983; Hirschman & Arons 2001b; Gallant et al 2002), the energy flux carried by the wind whilst close to the star is dominated by Poynting flux (Michel 1982). However, at the inner edge of the Crab Nebula, where the wind passes through a termination shock, it must have a very low magnetization, $\sigma \sim 10^{-3}$, if it is to match the observed expansion speed of the nebula (Rees & Gunn 1974; Kennel & Coroniti 1984; Emmering & Chevalier 1987) and the axial ratio of its optical isophotes (Begelman & Li 1992). Thus, unless the structure of

the termination shock is very different to that of a hydrodynamic shock, dissipation of the magnetic field in the flow must occur before the flow reaches this radius.

The wind of the Crab pulsar is driven by a rotating neutron star in which a non-axisymmetric magnetic field is embedded — often assumed to be an oblique magnetic dipole. Close to the equatorial plane, the magnetic field in the wind forms toroidal “stripes” of opposite polarity, separated by a current sheet (Coroniti 1990; Bogovalov 1999), as illustrated in Fig. 1. In principle, a dissipative process operating on the scale of the wavelength of the striped pattern is capable of annihilating the oscillating component, which, in the equatorial plane, corresponds to the entire magnetic field. But the rate at which dissipation proceeds is uncertain. Using a particular prescription in which the speed of the charge carriers attains the maximum value of c , Coroniti (1990) and Michel (1994) found for the case of the Crab pulsar that dissipation should be completed well inside the termination shock, which occurs at a radius of roughly $10^9 r_L$ (where $r_L = c/\Omega$ is the radius of the light-cylinder and Ω the angular velocity of the star). However, an important effect of dissipation is that it causes the flow to accelerate. As magnetic field energy is converted into heat, the plasma performs work on the expanding wind and converts the heat into kinetic energy. Because of the relativistic dilation of time, this effect, which was not included in the treatments of Coroniti (1990) and Michel (1994), leads to an apparent decrease in the rate of dissipation in the rest frame of the star [Lyubarsky & Kirk (2001) henceforth LK]. As a result, this rate of dissipation does not solve the σ -problem.

Physically, this approach to dissipation is based on a one-dimensional picture in that it corresponds to magnetic field annihilation in a current sheet that is uniform in the plane perpendicular to the radius vector. In reality, we might expect the sheet to break up into a large number of regions where dissipation proceeds via magnetic reconnection in flow patterns which are two or three dimensional in nature (see, for example Priest and Forbes 2000). In this case, the global effect on the flow can be found by (i) maintaining the assumption that dissipation is confined to a layer around the field reversal, but allowing the thickness of this layer to be determined by an estimate of the average dissipation rate based on the physics of reconnection and (ii) assigning to the layer an average energy density and pressure, related to each other by an effective equation of state. The prescription used by Coroniti (1990), Michel (1994) and Lyubarsky & Kirk (2001) is equivalent to setting the thickness of the dissipation layer equal to the gyro radius of the current carriers and using the equation of state of an ideal relativistic gas. This gives a reasonable lower limit, but other prescriptions have been proposed (Lyubarsky 1996; Drenkhahn 2002; Lyutikov & Uzdensky 2002). In this paper we argue that an *upper* limit to the reconnection rate can be implemented by limiting the expansion speed of the layer to that of sound in an unmagnetized gas. We present the global properties of reconnecting, spherically symmetric, relativistic winds, including the

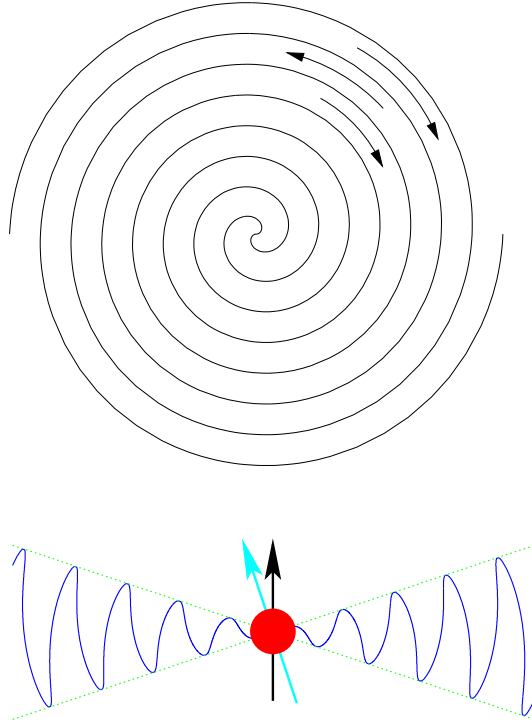


Fig. 1.— Top: The Parker spiral pattern in the equatorial plane. The arrows indicate the magnetic field direction of an obliquely rotating magnetic dipole, and the solid line gives the position of the current sheet. Bottom: the poloidal structure of the current sheet (thick, solid line). The arrows denote the spin axis (vertical) and magnetic dipole axis (inclined), and the thin line bounds the equatorial zone of the wind, in which magnetic reconnection is possible.

dependence of the Lorentz factor on radius, for each prescription. Our findings apply to any spherical relativistic flow that contains a toroidal field with radial fluctuations, but we phrase the discussion in terms of a pulsar wind, since this fixes the wavelength of the fluctuation as well as its initial amplitude. In the particular case of the Crab pulsar, we show that the σ -problem can be resolved if the initial value (i.e, the value at the fast magnetosonic point) of this parameter is at most 10^3 , or, equivalently, if the μ -parameter [see Eq. (23)] introduced by Michel (1969) is less than a few times 10^4 .

The paper is organized as follows: in Sect. 2 we review the equations derived by Lyubarsky & Kirk (2001) that describe, in the short wavelength limit, spherically symmetric MHD winds containing an oscillating component of the magnetic field which can undergo damping by dissipative effects. In Sect. 3 we discuss the modelling of the dissipative layer and describe how it can be incorporated into the MHD description. Section 4 contains a discussion of the various prescriptions for dissipation. In section 5, asymptotic solutions, valid for relativistic plasma temperatures, are found that give good approximations to the global properties of the flows, such as the radius at which dissipation is complete. These are compared to numerical solutions, which indicate the sensitivity to variations in the initial conditions, delineate regions in which the dissipation prescriptions become unphysical and quantify departures from the asymptotic solutions when the plasma temperature is nonrelativistic. We compute the effective diffusivity implied by our results in Sect. 6 and compare it to the Bohm diffusivity. The implications of our results, in particular for the Crab pulsar and its nebula, are discussed in Sect. 7 and a summary of our conclusions is presented in Sect. 8.

2. MHD equations in the short wavelength approximation

In this paper we investigate the evolution of a radial MHD wind containing a purely toroidal magnetic field. This idealisation is thought to be a reasonably good approximation in the case of a pulsar for radii far outside the light cylinder, $r \gg r_L$ [see, for example Coroniti (1990)]. However, alternative pictures in which the radial component of the magnetic field plays a role are possible (Kuijpers 2001). Following Lyubarsky & Kirk (2001) we consider the slow evolution of a periodic entropy wave, containing two reversals of the magnetic direction per oscillation, as it propagates outwards in the spherically symmetric wind. The flow pattern is assumed to be steady in the sense that at fixed radius the amplitude of the wave is constant in time, so that the flow variables are exactly periodic. The radial evolution is governed by two factors: the gradual annihilation of the oscillating component of the magnetic field embedded in the wave according to one of the microphysical prescriptions discussed in Sect. 4

and the expansion and acceleration of the plasma as a result of the spherical geometry and the outwardly directed force arising from the pressure gradient. The evolution of the wave is assumed to be slow — significant changes are permitted only over radial scales large compared to the wavelength ($= 2\pi r_L v/c$, where v is the bulk radial velocity). The equations describing the evolution are obtained from a perturbation expansion in the small parameter r_L/r and involves averaging over a wave period the equations of continuity, energy and entropy. The procedure is described in detail in LK. The zeroth order equations give the familiar conditions for the entropy wave mode: pressure equilibrium between plasma and magnetic field and zero bulk speed in the wave frame. Imposing non-secularity conditions on the first order equations then gives expressions governing the slow evolution of the zeroth order quantities. From the continuity equation one obtains:

$$\frac{\partial}{\partial r} (r^2 \gamma v \langle n' \rangle) = 0, \quad (1)$$

and from the energy equation:

$$\frac{\partial}{\partial r} \left(r^2 \gamma^2 v \left\langle e' + p' + \frac{B^2}{4\pi\gamma^2} \right\rangle \right) = 0. \quad (2)$$

The entropy equation includes ohmic dissipation to first order in r_L/r , and can be written in terms of the magnetic field, using Maxwell's equations:

$$\begin{aligned} & \frac{\langle e' + p' \rangle}{r^2} \frac{\partial}{\partial r} (r^2 \gamma v) \\ + \gamma v \frac{\partial}{\partial r} \langle e' \rangle + \frac{1}{4\pi\gamma r} \left\langle B \frac{\partial}{\partial r} (rvB) \right\rangle & = 0. \end{aligned} \quad (3)$$

In these expressions, gaussian units have been employed, the magnetic field and fluid velocity in the laboratory frame (in spherical polar coordinates) are $\vec{B} = B(r, t)\vec{\phi}$ and $\vec{v} = v(r, t)\vec{r}$ and the notation $\langle \cdot \rangle$ denotes an average over a wave period. The proper particle density is denoted by n' , the proper energy density e' is the component $T^{0,0}$ of the stress-energy tensor measured in the rest frame and the pressure p' refers to the radial component $T^{1,1}$ in the same frame.

3. The current sheet

In order to perform the averaging in Eqs. (1), (2) and (3) an explicit model of the entropy wave and the associated current is needed. Lyubarsky & Kirk (2001) used a fluid model in which a hot, unmagnetized plasma separates regions of opposing magnetic field

containing cold plasma. The transition at the interface of the hot and cold regions was assumed to be sharp. In this paper, we use instead an exact stationary solution of the full Vlasov/Maxwell kinetic equations that contains a magnetic field reversal. This solution also forms the basis of the discussion of the microphysics presented in Sect. 4. When an average over one wavelength is performed, the equations obtained are essentially the same as those used by Lyubarsky & Kirk (2001), with two minor differences. The first is connected with the presence of a cold plasma component within the hot parts of the sheet and is noted below where it appears. The second arises when the drift speed of the charge carriers is relativistic and it becomes necessary to compute the effective ratio of specific heats of the plasma as a function of position according to Eq. (A23). We expect this effect to be unimportant and do not investigate it in detail. The use of an equilibrium distribution presupposes an effective collision time t_{coll} that is short compared to the dynamical time t_{dyn} . On the other hand, each dissipation prescription has an associated value of t_{coll} . In Sect. 6 we show that indeed $t_{\text{coll}} < t_{\text{dyn}}$ in each case.

The exact stationary solution we use was originally found by Harris (1962) for the nonrelativistic case and subsequently generalized to apply also to the case of relativistic particle temperatures and drift speeds by Hoh (1968). It contains three parameters which can be chosen to be the magnetic field B'_0 far from the current sheet, the number density of particles of each charge N'_\pm at the center of the sheet and the sheet width a , each measured in a frame of reference in which the sheet is stationary and the electric field vanishes. One can then define a temperature T (in energy units) which is independent of position:

$$T = \frac{B_0'^2}{16\pi N_\pm'}. \quad (4)$$

The Debye length at the center of the sheet

$$\lambda_D = \left(\frac{T}{4\pi N_\pm' e^2} \right)^{1/2}, \quad (5)$$

is, to within a factor of the order of unity, equal to the gyro radius of a particle of energy T in the magnetic field B'_0 , provided $T \gg mc^2$. The sheet is neutral and the electric field vanishes everywhere. The current is carried by oppositely directed drifts of oppositely charged particles. Specialising to the case in which only positrons and electrons are present, the speed $\pm c\beta$ with which each component drifts is

$$\beta = \frac{\lambda_D}{a}, \quad (6)$$

and is independent of position in the sheet. The current sheet in this solution is planar, but can be used to describe each of the sequence of nested quasi-spherical sheets contained in the

radial wind, provided the sheet thickness remains small compared to the wavelength. The frame of reference used to portray the sheet solution is one which moves radially outwards with the bulk velocity of the wind. A derivation of the internal structure is presented in Appendix A. For a single sheet located at radius r at $t = 0$, the magnetic field $B'(r)$ and the density of each species of charge carrier n'_{\pm} are

$$B'(r, t) = B'_0(r) \tanh \left[\frac{\gamma vt}{a(r)} \right], \quad (7)$$

$$n'_{\pm}(r, t) = N'_{\pm}(r) \operatorname{sech}^2 \left[\frac{\gamma vt}{a(r)} \right], \quad (8)$$

An additional spatially uniform component of cold, neutral, current-free plasma of arbitrary density can be added to this solution without changing the above results. The solution is also unaffected by the addition of a constant magnetic field of arbitrary strength in the $\hat{\theta}$ direction.

One wavelength of the entropy wave contains two current sheets of opposite polarity. Defining the fraction Δ of the wave occupied by hot plasma as

$$\Delta = \frac{2ac}{\gamma\pi r_{\text{L}}v}, \quad (9)$$

and averaging over one wave period, one finds for the particle number density n' ($=2n'_{\pm}$):

$$\langle n' \rangle = 2N'_{\pm}\Delta + n'_c, \quad (10)$$

where n'_c is the density of the uniform cold background plasma. The average of the pressure p' follows from the stress-energy tensor of the sheet particles (Eq. A21)

$$\langle p' \rangle = 2N'_{\pm}\Delta T = \frac{B_0'^2}{8\pi}\Delta, \quad (11)$$

and this can be related to the average energy density by defining the effective ratio of specific heats $\hat{\gamma}$ according to

$$p' = (\hat{\gamma} - 1)(e' - n'mc^2), \quad (12)$$

[see Eq. (A23)]. In principle, $\hat{\gamma}$ is capable of accounting not only for potential anisotropies in the gas (p' refers to the r - r component of the stress-energy tensor — see Appendix A) but also for other non-equilibrium particle distributions, e.g., those of power-law type.

The magnetic field as given by Eq. (7) leads to

$$\left\langle \frac{B^2}{4\pi\gamma^2} \right\rangle = \left\langle \frac{B'^2}{4\pi} \right\rangle,$$

$$= \frac{B_0'^2}{4\pi} (1 - \Delta), \quad (13)$$

$$\begin{aligned} \left\langle B \frac{\partial}{\partial r} (rvB) \right\rangle &= \gamma^2 B_0'^2 (1 - \Delta) \frac{\partial}{\partial r} (rv) + \\ &\frac{rv}{2} \frac{\partial}{\partial r} \left[\gamma^2 B_0'^2 (1 - \Delta) \right]. \end{aligned} \quad (14)$$

Using these expressions, the (integrated) continuity and energy equations and the entropy equation (1, 2 and 3) become:

$$r^2 \gamma v (n'_c + 2N'_\pm \Delta) = \frac{2\dot{N}_\pm}{\Omega_w} \equiv \Phi, \quad (15)$$

$$\gamma mc^2 \Phi + r^2 \gamma^2 v \frac{B_0'^2}{8\pi} \left[2 + \left(\frac{2 - \hat{\gamma}}{\hat{\gamma} - 1} \right) \Delta \right] = \frac{L}{\Omega_w} \equiv \Psi, \quad (16)$$

$$\begin{aligned} &\left(\frac{\hat{\gamma}}{\hat{\gamma} - 1} \right) \frac{B_0'^2 \Delta}{8\pi r^2} \frac{\partial}{\partial r} (r^2 \gamma v) + \\ &\gamma v \frac{\partial}{\partial r} \left(\frac{\Delta}{\hat{\gamma} - 1} \frac{B_0'^2}{8\pi} \right) + \frac{v}{\gamma} \frac{\partial}{\partial r} \left[\gamma^2 (1 - \Delta) \frac{B_0'^2}{8\pi} \right] \\ &+ \frac{\gamma B_0'^2 (1 - \Delta)}{4\pi r} \frac{\partial}{\partial r} (rv) = 0, \end{aligned} \quad (17)$$

where \dot{N}_\pm is the rate at which pairs leave the star (corresponding to $2\dot{N}_\pm$ particles per second) and L is the luminosity in the wind, which is assumed to occupy a solid angle Ω_w . The constants Φ and Ψ represent the particle flux and the total energy flux.

These equations are complemented by the condition that far from the center of the current sheets the magnetic flux remain frozen into the plasma:

$$\frac{B_0'}{rn'_c} = \text{constant}. \quad (18)$$

We now define the fraction ξ of particles carried in the hot plasma:

$$\xi = \frac{2N'_\pm \Delta \gamma v r^2}{\Phi}, \quad (19)$$

and a dimensionless quantity \hat{p} that is related to the magnetic pressure in the cold part of the wind:

$$\hat{p} = \frac{r^2 \gamma^2 v B_0'^2}{4\pi \Psi}. \quad (20)$$

The continuity equation then simply relates the density of cold plasma n'_c to ξ :

$$\xi + \frac{\gamma v r^2 n'_c}{\Phi} = 1, \quad (21)$$

and the energy equation becomes

$$\frac{\gamma}{\mu} + \left[1 + \frac{2 - \hat{\gamma}}{2(\hat{\gamma} - 1)} \Delta \right] \hat{p} = 1, \quad (22)$$

where the constant μ is the total energy carried by the wind per unit rest mass ($\times c^2$):

$$\mu = \frac{\Psi}{m c^2 \Phi} = \frac{L}{2 \dot{N}_{\pm} m c^2}, \quad (23)$$

as introduced by Michel (1969). Physically, $(1 - \Delta) \hat{p}$ is the fraction of the wind luminosity carried by magnetic field, γ/μ is the fraction carried by the particle rest mass and the remainder, $\hat{p} \hat{\gamma} \Delta / [2(\hat{\gamma} - 1)]$, can be attributed to the enthalpy flux. The constant μ is related to the more commonly used σ (Kennel & Coroniti 1984; Kirk & Duffy 1999), defined as the ratio of Poynting flux to particle-born energy flux by

$$\sigma = (1 - \Delta) \hat{p} \left[\frac{\gamma}{\mu} + \left(\frac{\hat{\gamma}}{\hat{\gamma} - 1} \right) \hat{p} \Delta \right]^{-1}, \quad (24)$$

where σ is, in general a function of r , but is constant in cold ($\Delta = 0$), spherically symmetric flows of constant speed, in which case $\sigma = \mu \hat{p} / \gamma \approx \mu / \gamma$, for $\mu \gg 1$.

The entropy equation is

$$\begin{aligned} & \left(\frac{2 - \hat{\gamma}}{\hat{\gamma} - 1} \right) \frac{d\Delta}{d \ln r} + \left[1 + \left(\frac{2 - \hat{\gamma}}{\hat{\gamma} - 1} \right) \Delta \right] \frac{d \ln \hat{p}}{d \ln r} \\ & + \left[\frac{c^2}{\gamma^2 v^2} - \left(\frac{2 - \hat{\gamma}}{\hat{\gamma} - 1} \right) \Delta \right] \frac{d \ln \gamma}{d \ln r} + 2\Delta = 0, \end{aligned} \quad (25)$$

in which, for simplicity, we have assumed $\hat{\gamma}$ is constant, and the condition of flux freezing in the cold part of the flow is

$$\frac{\hat{p} v}{(1 - \xi)^2} = \text{constant}. \quad (26)$$

Thus the conservation equations and the entropy equation yield three equations (22), (25) and (26) in the four unknowns ξ , γ , \hat{p} and Δ .¹

¹The current sheet model adopted by Lyubarsky & Kirk (2001) does not allow cold and hot components of the particle distribution to coexist at the same position. This leads to a slightly different expression for the density of cold particles: $\xi + \gamma v r^2 n'_c (1 - \Delta) / \Phi = 1$, instead of Eq. (21), and, consequently for the flux freezing condition: $\hat{p} (1 - \Delta)^2 v / (1 - \xi)^2 = \text{constant}$, instead of Eq. (26).

To close this set, it is necessary to specify the rate at which dissipation occurs using one of the prescriptions discussed below. An additional physical constraint on these can be found by requiring that the ohmic dissipation term in the entropy equation be positive. Performing the perturbation expansion as indicated above and described in Appendix B, this gives the condition

$$\frac{d}{d \ln r} \left[\hat{p}^{1/\hat{\gamma}} (r^2 v / \gamma^2)^{(\hat{\gamma}-1)/\hat{\gamma}} \Delta \right] > 0. \quad (27)$$

4. Dissipation prescriptions

In the following, three different prescriptions for the effective, globally averaged rate of dissipation are introduced. Each prescription has a specific, physical motivation and corresponds in a resistive MHD analogy to a certain value for the effective magnetic diffusivity, as discussed in Sect. 6.

4.1. Slow dissipation

The current sheet described above can be realized only if the drift speed required by Eq. (6) is subluminal. This gives an absolute lower limit on the thickness of the sheet, or alternatively, on the fraction of particles it contains. The Debye length can be written as:

$$\frac{\lambda_D}{a} = \frac{\mu r}{r_L \xi \gamma} \left(\frac{\hat{p} v}{\hat{L} c} \right)^{1/2}, \quad (28)$$

where we have defined the dimensionless flow luminosity

$$\hat{L} = \left(\frac{\pi^3 e^2 \Psi}{m^2 c^5} \right). \quad (29)$$

Then the condition for a subluminal drift speed, $\beta \leq 1$, becomes

$$\xi \geq \xi_{\min} = \frac{\mu r}{r_L \gamma} \left(\frac{\hat{p} v}{\hat{L} c} \right)^{1/2}. \quad (30)$$

The treatments of both Coroniti (1990) and Michel (1994) amount to setting $\xi = \xi_{\min}$. Lyubarsky & Kirk (2001) also used this condition. A current sheet with particle distributions that are in equilibrium does not, of course, dissipate magnetic energy. However, as the sheet moves outwards with the flow, the parameters describing it change and it is this slow evolution through a sequence of quasi-equilibria which implies dissipation. Eq. (30) leads to a lower limit on the dissipation rate, since a larger value of ξ implies a thicker sheet (larger Δ) and smaller fraction of the total energy flux carried by the fields.

4.2. Fast dissipation

The maximum dissipation rate is more difficult to estimate. It follows from the maximum speed at which the current sheet can expand into the surrounding plasma and still remain in the neighbourhood of the Harris equilibrium. Denoting this speed by $c\beta_c$ (> 0), the associated rate of evolution of the sheet thickness with radius, can be written:

$$\frac{d\Delta}{d \ln r} = \frac{2\beta_c r c^2}{\pi r_L \gamma^2 (v^2 - c^2 \beta_c^2)}, \quad (31)$$

(see Appendix C).

In the outer parts of the sheet, the balance between magnetic and particle pressure can no longer be maintained if the bulk velocity exceeds the local speed of the fast magnetosonic mode $c\beta_f$. This suggests the condition

$$\begin{aligned} \beta_c &\leq \beta_f = \sqrt{\frac{B'^2/4\pi}{n'_c m c^2 + B'^2/4\pi}}, \\ &= \left[1 + \frac{\gamma}{\mu \hat{p}} (1 - \xi) \right]^{-1/2}. \end{aligned} \quad (32)$$

Drenkhahn (2002) has generalized this prescription, introducing a parameter $\epsilon = \beta_c/\beta_f$ and arguing that it is typically of the order of unity.

However, in the absence of a component of the magnetic field in the $\vec{\theta}$ direction, the Harris equilibrium has at its center a neutral layer. This can only be maintained close to equilibrium if the expansion speed is small compared to the sound speed in the unmagnetized gas. Were this not the case, the layer would lose its internal pressure support and be crushed by the external magnetic pressure. In the case of a relativistic temperature ($T \gg mc^2$) this leads to the condition

$$\beta_c \leq \frac{1}{\sqrt{3}}. \quad (33)$$

In the outer parts of the flow, where the plasma temperature decreases to below the electron rest mass, condition (33) is inapplicable and for $T \ll mc^2$, the sound speed is $\sqrt{\hat{\gamma}T/(mc^2)}$. A full treatment of the dynamics in this regime requires a local evaluation of the equation of state, i.e., of the effective ratio of specific heats $\hat{\gamma}$. In this paper, we avoid such complications by taking $\hat{\gamma} = 4/3$ everywhere in the current sheet, which is appropriate for any isotropic gas in which the particles are relativistic ($E \approx cp$). Nevertheless, we can take approximate account of a more realistic sound speed by setting

$$\beta_c \leq \text{Min} \left(\frac{1}{\sqrt{3}}, \sqrt{\frac{T}{mc^2}} \right). \quad (34)$$

In flows in which the Poynting flux dominates, this restriction leads to a much more stringent upper limit on the dissipation rate than does Eq. (32), since $\beta_f \approx 1$, for $\sigma \gg 1$, and the denominator on the right-hand side of Eq. (31) becomes small. The limit can be relaxed slightly if an additional component of the magnetic field (in the $\vec{\hat{\theta}}$ direction) is present in the sheet. In this case the local speed of the fast mode would be more appropriate than the speed of sound in an unmagnetized plasma. However, this makes only a minor difference, provided the plasma at the center of the sheet is not too far from equipartition.

4.3. Dissipation limited by the tearing mode

The Harris equilibrium is well-known to be unstable to the excitation of a variety of waves in the non-relativistic case — see, for example, Daughton (1999); Biskamp (2000). It is thought that the current sheet first filaments because of the growth of the tearing mode, producing magnetic islands separated by neutral lines. These then lead to magnetic reconnection and its associated dissipation (Melrose 1986). This scenario has largely been developed in the context of the geomagnetic tail of the Earth. Particle-in-cell simulations appear to confirm its validity (Zhu & Winglee 1996; Pritchett et al. 1996), although the 3-dimensional picture is more complicated (Büchner & Kuska 1999; Hesse et al. 2001)

In the relativistic case the linear growth rate of the tearing instability has been calculated by Zelenyi & Krasnosel'skikh (1979). For $T \gg mc^2$ they find for the most unstable mode, which has a wavelength approximately equal to the sheet thickness,

$$\begin{aligned} \gamma_t &= \beta^{3/2} c/a, \\ &= \lambda_D^{3/2} c/a^{5/2}. \end{aligned} \tag{35}$$

Thus, for a given number of particles in the sheet, and fixed external pressure (implying ξ , \hat{p} and β constant), the growth rate is faster for thinner sheets. Lyubarsky (1996), in his model of the high energy emission from the Crab pulsar, suggested that the speed β_c of expansion of the sheet could be self-regulating being governed by the fastest growing mode of the relativistic collisionless tearing mode instability:

$$\beta_c = a\gamma_t/c, \tag{36}$$

or, in terms of the flow variables,

$$\frac{d(\gamma\Delta)}{d \ln r} = \frac{2rc}{\pi r_L \gamma v} \left(\frac{\xi_{\min}}{\xi} \right)^{3/2}. \tag{37}$$

5. Solutions of the flow equations

In this section we estimate both the length scale on which dissipation converts an initially Poynting-dominated flow into one in rough equipartition, as well as the rate at which the flow accelerates, i.e., $\gamma(r)$ during this process. To simplify the results, we specialize to the case of a relativistic gas: $\hat{\gamma} = 4/3$.

At an initial radius, assume the flow contains a thin sheet $\Delta \ll 1$ containing relatively few particles $\xi \ll 1$, is Poynting flux dominated with $\gamma/\mu \ll 1$ and already super magnetosonic $\gamma > \mu^{1/3}$. As the radius increases, the flow accelerates, but, as long as the above ordering is maintained, we may set $\hat{p} \approx 1$ and $v \approx c$. In this range, the flux freezing equation (26) reduces to the approximate relation

$$\frac{\gamma}{\mu} - 2\xi + \Delta = \text{constant}, \quad (38)$$

and the entropy equation is

$$\frac{d}{d \ln r} \Delta - \left(2\Delta + \frac{\gamma}{\mu} \right) \frac{d}{d \ln r} \ln \gamma + 2\Delta = 0. \quad (39)$$

When these two equations are complemented by one of the dissipation prescriptions [using, for fast dissipation, Eq. (33)], it is straightforward to obtain asymptotic solutions for the flow for large radius. These take the form

$$\Delta \propto r^q, \quad (40)$$

$$\xi = \frac{\Delta}{q}, \quad (41)$$

$$\frac{\gamma}{\mu} = \frac{\Delta(2-q)}{q}, \quad (42)$$

[or, in the case of the LK sheet, $\xi = \Delta(1+q)/q$ instead of Eq. (41)]. Shortly before dissipation is complete, at the point where \hat{p} decreases, $\Delta \approx \xi \approx 1$ and $\gamma \approx \mu$, the solutions lose their validity. For each dissipation prescription, the asymptotic solutions yield reasonably accurate estimates of the radius at which this occurs, as well as the dependence of the flow variables on radius up to this point. An estimate of the smallest radius at which the asymptotic solutions are valid is obtained by locating the magnetosonic point. These results are summarized in Table 1. The radius at which dissipation is complete can be estimated by inserting into the asymptotic solution either $\Delta = 1$, $\xi = 1$, or $\gamma = \mu$ and the numerical integrations indicate that the latter is somewhat more accurate. Table 1 gives this radius with a numerically estimated coefficient to order of magnitude accuracy. For slow dissipation this asymptotic

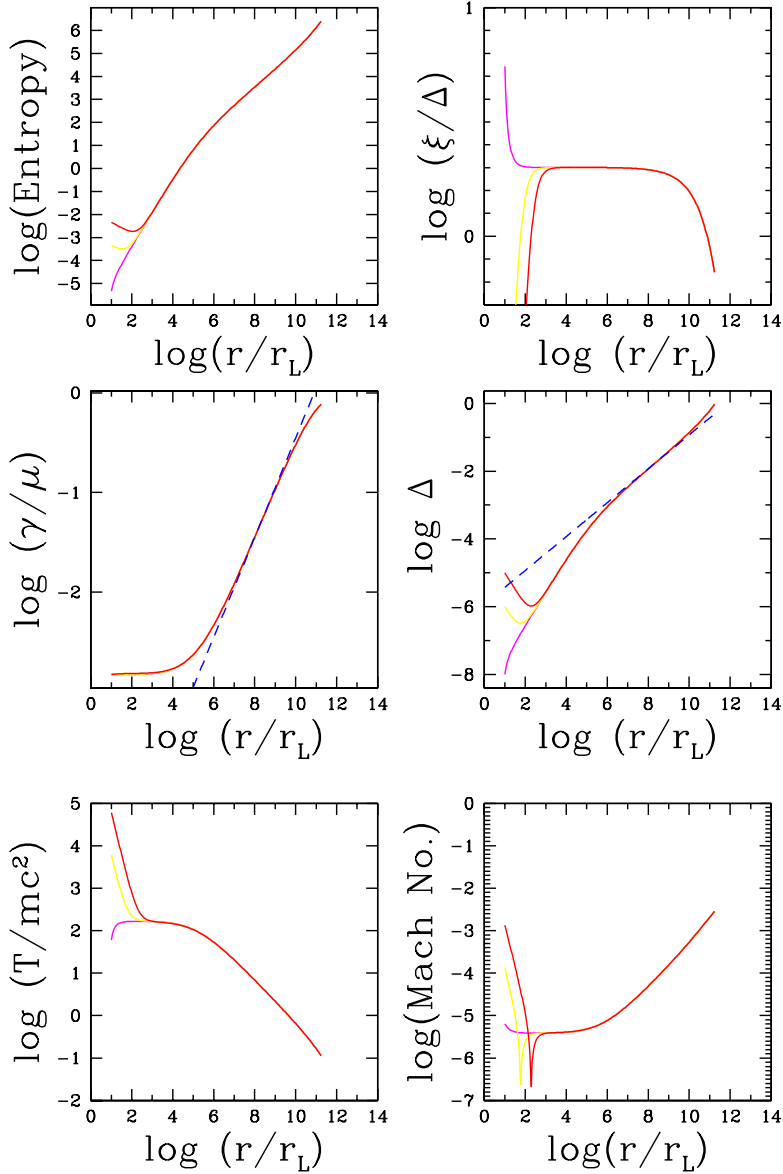


Fig. 2.— The flow variables as functions of radius for slow dissipation and parameters $\hat{L} = 1.5 \times 10^{22}$, $\Omega_w = 4\pi$, $\mu = 2 \times 10^4$, thought appropriate for the Crab pulsar. Displayed are the average entropy [see Eq. (27)], the bulk Lorentz factor, the fraction of a wavelength occupied by the hot sheet Δ , the temperature and the Mach number of the expansion speed of the sheet. The top right panel shows the ratio ξ/Δ (which gives the ratio between the density of hot particles in the sheet, and the wavelength-averaged density of both hot and cold particles). Three numerical solutions are shown as solid lines for different initial conditions on Δ . The asymptotic solutions for γ and Δ are shown as dashed lines.

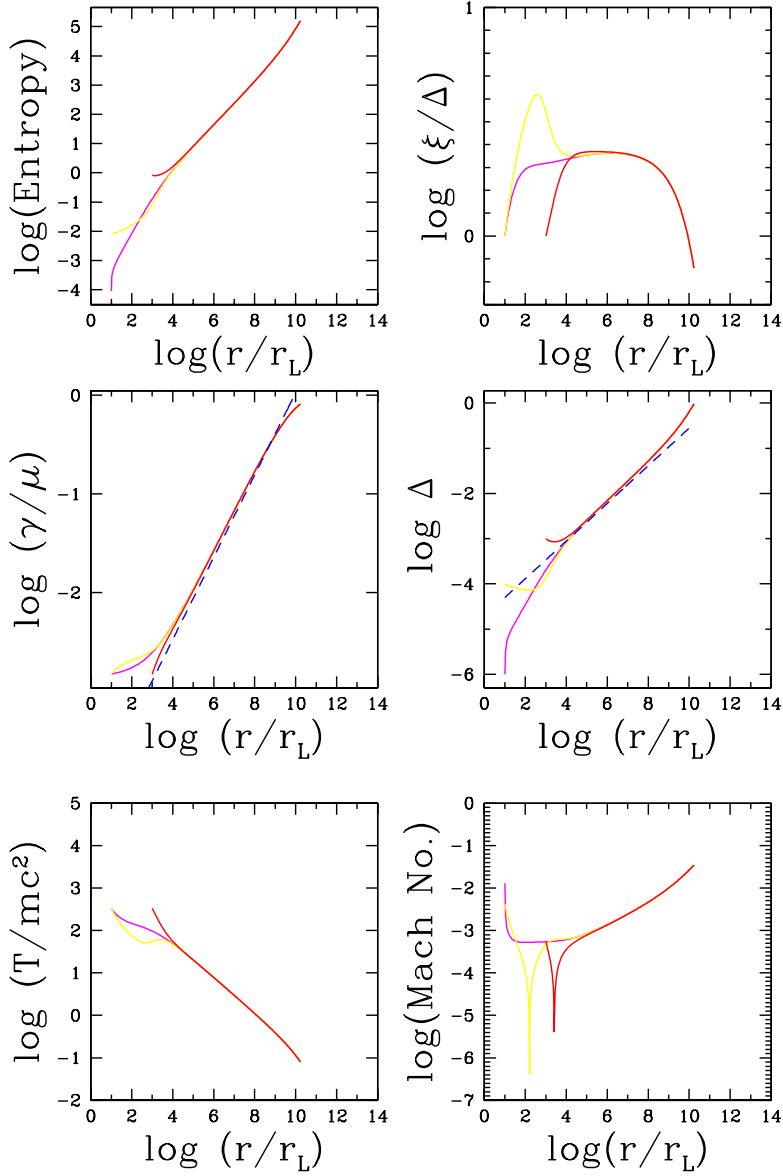


Fig. 3.— The flow variables as functions of radius for tearing mode limited dissipation (parameters as in Fig. 2). Three solutions are shown as solid lines for initial conditions $\Delta = 10^{-6}$ and 10^{-4} starting at $r = 10r_L$, and for $\Delta = 10^{-3}$ starting at $r = 1000r_L$. The asymptotic solution is shown as a dashed line.

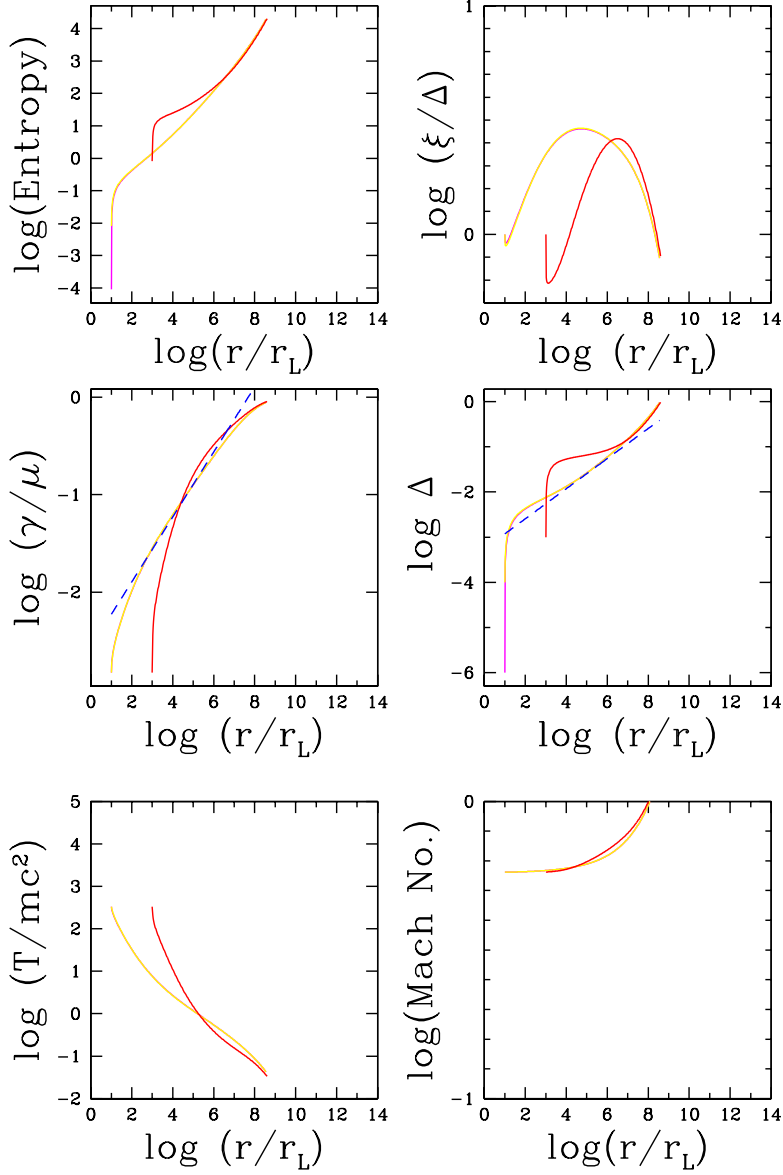


Fig. 4.— The flow variables as functions of radius for fast dissipation according to Eqs. (31) and (33), for the same parameters and initial conditions as in Fig. 3. The solutions with initial values of $\Delta = 10^{-6}$ and $\Delta = 10^{-4}$ coincide for almost all radii.

solution was originally found by Lyubarsky & Kirk (2001); for fast dissipation, the scaling with radius agrees with that given by Drenkhahn (2002).

Figure 2 compares the results of a numerical integration of the full equation set, Eqs. (22), (25) and (26), together with the prescription for slow dissipation in which ξ is required to equal ξ_{\min} , defined in Eq. (30). The parameters chosen in this and the following three figures are those implied by the discussion of the Crab pulsar in Sect. 7: $\hat{L} = 1.5 \times 10^{22}$ and $\mu = 2 \times 10^4$. Six quantities are plotted against radius:

1. the quantity defined in Eq. (27) which is proportional to the entropy averaged over a wavelength
2. the ratio ξ/Δ , that is the ratio of the density of hot particles to the wavelength-averaged particle density
3. the Lorentz factor γ (in units of its maximum value μ)
4. the fraction Δ of a wavelength occupied by hot plasma
5. the temperature
6. the absolute value of the Mach number (with respect to the fast magnetosonic speed in the cold part of the wind) with which the sheet expands.

Solutions are shown for three different sets of initial conditions with $\Delta = 10^{-8}$, 10^{-6} and 10^{-5} , all starting at the point $r = 10r_L$ with a slightly supermagnetosonic Lorentz factor $\gamma = 1.1\mu^{1/3} \approx 33$. All converge rapidly to the asymptotic solution given in Table 1 and Eqs. (40-42), which, in the case of γ and Δ , is plotted as a dashed line. Deviations from this solution are small and appear only close to the maximum radius, where dissipation is complete. Using this prescription for dissipation, it is possible to choose an arbitrarily small initial value of Δ — the results do not differ appreciably from the case $\Delta = 10^{-8}$. However, these solutions adjust rapidly in the initial phase and cannot strictly be described by the perturbation approach underlying our method, which assumes all variations to be on a length scale equal to or larger than the local radius. For the larger initial values of Δ , the region occupied by hot plasma shrinks as the flow moves outwards. This is accompanied by a decrease in the averaged entropy, indicating that the prescription is unphysical. Thus, we cannot be sure that initial states with such a large value of Δ will approach the asymptotic solution, since a different dissipation prescription with increased entropy generation is required at least initially. Different values of the starting point in radius yield qualitatively similar solutions.

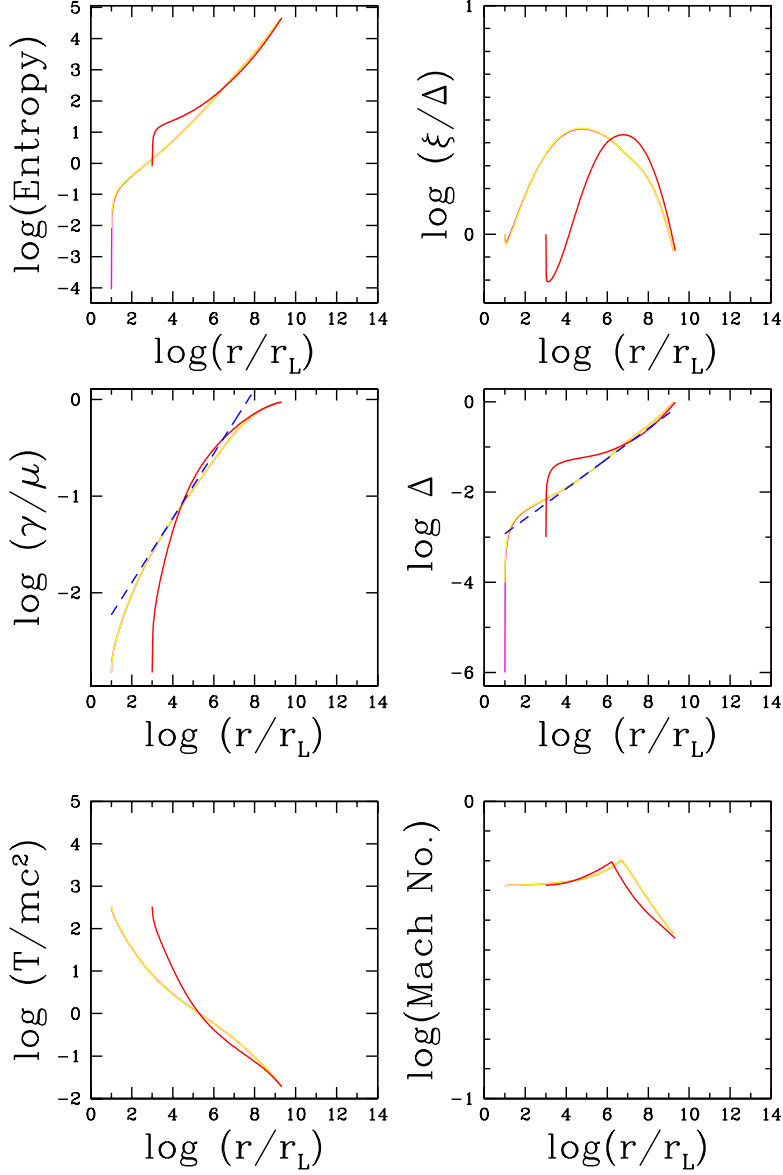


Fig. 5.— The flow variables as functions of radius for fast dissipation using a realistic estimate of the sound speed according to Eq. (34), and for the same parameters and initial conditions as in Fig. 4. The solutions with initial conditions $\Delta = 10^{-6}$ and $\Delta = 10^{-4}$ coincide for almost all radii.

Figure 3 shows results for the case of tearing mode limited dissipation, Eq. (37). Three different sets of initial conditions were chosen: $\Delta = 10^{-6}$ and 10^{-4} starting at $r = 10r_L$ and $\Delta = 10^{-3}$ starting at $r = 1000r_L$. Because this prescription takes the form of a first order differential equation, an additional initial condition on ξ is needed — we choose $\xi = \Delta$. Once again, the asymptotic solution provides a reasonable approximation at large radius. In this case, however, the entropy increases in all solutions, despite the fact that the region occupied by hot plasma shrinks slightly. Thus, this prescription provides a physically consistent description of the approach of the flow to the asymptotic solution even for quite large initial values of Δ . However, the initial density contrast ξ/Δ between the hot and cold parts of the flow has to be chosen with some care in order to avoid rapidly varying transients. At $r > 10^8 r_L$, the plasma temperature is nonrelativistic, $T < mc^2$ and the expression used for the growth rate of the tearing mode instability loses validity.

The case of fast dissipation is shown in Fig. 4, where we have used the relativistic sound speed (33) as an upper limit on the expansion rate of the sheet. Here again, the dissipation prescription takes the form of an ordinary differential equation, so that initial conditions on both Δ and ξ are required. These were chosen to be the same as those of Fig. 3. The solutions again converge to the asymptotic expressions, and the entropy rises throughout. However, the initial transients fluctuate more strongly here than in the case of the tearing mode limited prescription. The result of the more realistic estimate of the sound speed given by Eq. (34) is shown in Fig. 5, for the same parameters and initial conditions as used in Fig. 4. Differences between these two sets of solutions appear only in the outer parts of the flow, where the temperature of the plasma becomes nonrelativistic. The Mach number drops sharply at this point, and the dissipation rate is reduced. Independent of the initial conditions, the solutions terminate at $r \approx 2 \times 10^9 r_L$. No asymptotic solutions are available to describe this outer phase of the flow. Nevertheless, the estimates of the radius at which dissipation is complete obtained using the asymptotic solutions for fast reconnection given in Table 1 remain accurate to within roughly an order of magnitude.

6. Comparison with dissipation by Bohm diffusion

For each dissipation prescription, the effective relaxation time of the plasma can be estimated by appealing to an MHD picture: the magnetic diffusivity η is related to the sheet thickness and the dynamical evolution time in the comoving frame t_{dyn} by

$$\eta \approx \frac{a^2}{t_{\text{dyn}}} \quad (43)$$

and is given in terms of the effective collision time t_{coll} by

$$\eta = \frac{\lambda_{\text{D}}^2}{t_{\text{coll}}}, \quad (44)$$

where we have used λ_{D} instead of the Larmor radius, as appropriate in a relativistic plasma (in the current model the two differ by a constant factor of the order of unity). Combining these two equations gives

$$t_{\text{coll}} \approx \left(\frac{\lambda_{\text{D}}}{a}\right)^2 t_{\text{dyn}} \quad (45)$$

and we see that the collision time is shorter than the dynamical time provided $a > \lambda_{\text{D}}$, or equivalently, $\xi > \xi_{\text{min}}$.

As can be seen from Eq. (40), the asymptotic solutions presented in Sect. 5 correspond to a dynamical timescale for the current sheet in the comoving frame given, to within a factor of the order of unity, by

$$t_{\text{dyn}} = \frac{r}{\gamma c}. \quad (46)$$

Thus, it is straightforward to compare the effective collision time implied by the dissipation prescription t_{coll} with the relaxation time $t_{\text{B}} \approx \lambda_{\text{D}}/c$ corresponding to “Bohm” diffusivity in a relativistic plasma. Using Eqs. (45) and (28), we have

$$\begin{aligned} \frac{t_{\text{coll}}}{t_{\text{B}}} &\approx \left(\frac{\lambda_{\text{D}}}{a}\right) \left(\frac{r}{r_{\text{L}}\Delta\gamma^2}\right), \\ &= \frac{\mu r^2}{\xi\gamma^3 r_{\text{L}}^2 \Delta} \left(\frac{\hat{p}v}{\hat{L}c}\right)^{1/2}. \end{aligned} \quad (47)$$

At the outer radius, this ratio takes on its smallest value for slow dissipation and for dissipation limited by the tearing mode:

$$\frac{t_{\text{coll}}}{t_{\text{B}}} \gtrsim \begin{cases} \left(\hat{L}^{1/4}/\mu\right)^2 & \text{(slow)} \\ \left(\hat{L}^{1/4}/\mu\right)^{2/5} & \text{(tearing mode)} \end{cases} \quad (48)$$

and its largest value for fast dissipation:

$$\frac{t_{\text{coll}}}{t_{\text{B}}} \lesssim \left(\frac{\hat{L}^{1/4}}{\mu}\right)^{-2} \quad \text{(fast)}. \quad (49)$$

7. Discussion

For the acceleration of the flow to proceed as we have described, the actual dissipation rate must lie above that of ‘slow’ dissipation and below that of ‘fast’ dissipation. To a reasonable approximation, these conditions can be imposed simply by inspecting the appropriate values of r_{\max} and r_{\min} , as given in Table 1. It is immediately clear that no prescription can fulfil these requirements unless μ is less than a certain maximum value. Adopting $\beta_c = 1/\sqrt{3}$, we find

$$\mu < 3\hat{L}^{1/4} . \quad (50)$$

Physically, restriction (50) arises because at higher values of μ the sheet would have to expand supersonically in order to accumulate enough particles to maintain the required current. This restriction was pointed out by LK, who speculated that, when it is violated, dissipation ceases before the available magnetic energy is exhausted. Whether this is the ultimate fate of such a wind is not completely clear. It is certainly true that our treatment using the Harris sheet or a model with hot and cold fluids fails in this regime, and it seems probable that no equilibrium can then exist in which the electric field vanishes in the comoving frame. Perhaps at this point it is essential to allow the conversion of the entropy wave into an electromagnetic mode, along the lines suggested by Melatos (2002).

If Eq. (50) is fulfilled, Eqs. (48) and (49) show that our solutions imply slower dissipation than the Bohm value at all radii for the ‘slow’ and ‘tearing-mode’ cases, but faster-than-Bohm dissipation in the ‘fast’ case. In standard treatments of reconnection, this value is often taken as an upper limit for the diffusivity (Somov & Titov 1985; Priest & Forbes 2000; Lyutikov & Uzdensky 2002). A higher value is justified, however, if the effective internal diffusion scale in the current sheet is given by a turbulent mixing length, rather than the characteristic Larmor radius of the particles. A turbulent sheet structure arises if the sheet filaments into a large number of reconnection centers when field dissipation begins. In the model presented here, it is assumed that the global sheet evolution can nevertheless be described within an MHD framework, using an effective average value for the dissipation rate.

As the wind approaches the point where dissipation is complete, the plasma temperature drops, as can be seen from Figs. 2–5, and the approximation of a relativistic gas fails. One effect of this is to invalidate our choice of a fixed ratio of specific heats $\hat{\gamma} = 4/3$ for the gas dynamics. However, more importantly, the dissipation prescriptions we have used are also affected. The Harris equilibrium gives a general expression for the drift speed of particles in the sheet, valid in both the relativistic and nonrelativistic cases, so that the prescription for slow dissipation remains a lower limit. The upper limit given by the limiting the speed

of expansion of the sheet to that of sound in an unmagnetized gas can also be implemented in the nonrelativistic case, as discussed in Sect. 4.2 and shown in Fig. 5. However, in the case of dissipation limited by the growth rate of the tearing mode, the physical basis of our estimates is no longer valid once the plasma temperature drops below the particle rest mass. An improved treatment, using an expression for the growth rate valid in the transrelativistic and nonrelativistic regimes is possible, but our estimates are in any case very rough, and the added complications would not appear to be justified.

However, given that sufficient particles are present in the wind to satisfy condition (50), and neglecting the modification of the tearing mode growth rate for nonrelativistic plasma, the prescription for tearing mode limited dissipation automatically lies between the limiting dissipation rates and can therefore be considered as a physically realistic possibility. For Crab pulsar parameters, $\hat{L} = 1.5 \times 10^{22}$ and condition (50) gives $\mu < 10^6$, for $\beta_c = 1/\sqrt{3}$. Estimates of the μ parameter for the Crab, based on modelling the X-ray and gamma-ray emission (Hibschman & Arons 2001a), exceed this value. In this case the solution obtained by LK for slow dissipation loses its validity before dissipation is complete. Nevertheless, the range of validity extends from close to the pulsar to well beyond the radius at which a termination shock is indicated by observations. X-ray observations (Weisskopf et al 2000) place this at a radius of 0.14 pc or $r = 2.7 \times 10^9 r_L$ in the equatorial plane. Slow dissipation implies steady acceleration of the wind to beyond this radius, without significant dissipation of the Poynting flux.

Recently, however, two different lines of investigation have suggested that the conventional approach seriously underestimates the rate at which pairs are injected by the Crab pulsar into its surrounding Nebula. Gallant et al (2002) have proposed a model that accounts for the synchrotron spectrum of the Nebula from the radio to hard gamma-ray bands. In particular, the large number of radio-emitting electrons, which could not be explained in the model of Kennel & Coroniti (1984), arise naturally from a relatively low speed, high density pulsar wind. The estimated injection rate is $\dot{N}_{\pm} \approx 3 \times 10^{40} \text{ s}^{-1}$, implying $\mu \approx 2 \times 10^4$. Lyubarsky & Eichler (2001), who analysed the dynamics of the X-ray jet, also conclude that a relatively low value of σ at the base of the flow is required. Because of the difficulty of collimating a very low density wind, they suggest that on the equator $\sigma < 10^2$. For a transonic wind, this implies $\mu = 10^3$.

Such low values of μ and the corresponding high pair densities, have important implications for dissipation in the pulsar wind. Firstly, independent of the actual mechanism, the asymptotic Lorentz factor of the wind after dissipation equals μ . This fits in well with the spectral modelling of Gallant et al (2002), who correlate this value with the break at 10^{16} Hz in the UV spectrum of the Crab Nebula. Secondly, although the radius at which

dissipation is complete is independent of μ in the ‘slow’ dissipation prescription of Coroniti (1990), Michel (1994) and LK, this is not true of the faster tearing mode limited case. From Table 1 it is evident that for $\mu = 2 \times 10^4$, dissipation by the tearing mode limited mechanism is still not complete within the termination shock. However, a faster mechanism could provide the required dissipation in this case. The lower limit on the dissipation radius implied by the estimates in Table 1 is $5 \times 10^7 r_L$ and Fig. 5 shows that when this limit is modified to take account of the nonrelativistic sound speed, the solution dissipates the magnetic field completely at $r = 2 \times 10^9 r_L$, i.e., within the termination shock. Adopting the value $\mu = 10^3$, or lower, reduces the dissipation radius still further, giving, for the tearing mode limited prescription, $r = 10^9 r_L$. The minimum distance required to dissipate the magnetic field into relativistic plasma according to Table 1 is $r > 1.5 \times 10^5 r_L$, and a numerical integration using the more general limit implied by Eq. (34) gives $r > 5 \times 10^6 r_L$.

It is interesting to note that the appearance of a dissipative wind may differ between these two cases. Kirk et al (2002) derived the criterion $\gamma^2 > r/r_L$ for the radiation emitted at a given radius in a striped wind to appear pulsed to the observer. Accordingly, for fast dissipation, radiation emitted by the hot current sheet at all positions within the flow should appear pulsed. On the other hand, the situation for dissipation limited by the tearing mode growth rate is more complicated: radiation from close to the maximum radius should not appear pulsed. However, nearer to the star the Lorentz factor of the flow is sufficient to ensure a pulsed appearance. The magnetic field in the flow decreases with increasing radius, so that the efficiency of conversion of heat into synchrotron radiation should be greater at smaller r . Consequently, pulsed radiation can be expected also in the tearing mode limited case.

8. Conclusions

We model the dissipation of an oscillating, toroidal magnetic field component in a relativistic MHD outflow by considering the radial evolution of the entropy wave associated with this pattern. Because of magnetic reconnection, or, more precisely, annihilation, plasma in the current sheets separating regions of oppositely directed field is heated. We assign an energy density and pressure to the sheets and relate them by the equation of state of a relativistic gas. Upon expanding, the sheet performs work, which causes the outflow to accelerate.

Despite recent progress (Zenitani & Hoshino 2001; Lyutikov & Uzdensky 2002) the dissipation rate in a relativistically hot pair plasma embedded in stripes of cold, magnetized plasma cannot be written down a priori. Thus, we consider three different prescriptions,

each with a specific physical motivation. A lower limit on the dissipation rate is given by the prescription used by Coroniti (1990), Michel (1994) and LK, in which the characteristic drift speed in the current sheet is equal to the speed of light (to within a factor of order unity). We argue that an upper limit on the dissipation rate is set by allowing the sheet to grow at its internal sound speed (in the comoving frame). When consistent with these limits, a physically plausible estimate of the actual rate is given by assuming that expansion of the current sheet is limited by the growth rate of the relativistic collisionless tearing mode. Comparing our prescriptions to a collisional MHD model, we find that the required dissipation is slower than the Bohm value when dissipation is limited by the tearing mode, but faster when the sheet grows at its internal sound speed. However, the complex flow pattern which will presumably be built up in the dissipation region make it difficult to draw conclusions from this analogy.

Analytic, asymptotic solutions, valid for relativistic plasma temperatures, are found for each prescription. These agree with and extend those presented by LK for slow dissipation, with $\gamma \propto r^{1/2}$, and by Drenkhahn (2002) for fast dissipation, with $\gamma \propto r^{1/3}$. For tearing-limited reconnection we find $\gamma \propto r^{5/12}$. Numerical integration of the full equation set confirms these solutions and demonstrates that they are valid until dissipation is nearly complete, although the dissipation rate in the fast prescription slows down once the plasma temperature becomes nonrelativistic. In general, transients associated with the initial conditions vanish rapidly. However, these transients reveal that for some initial conditions the slow dissipation prescription is unphysical in that it fails to create entropy.

Using the asymptotic solutions, the radius at which the oscillating part of the magnetic field is completely dissipated can be estimated in terms of the magnetization parameter μ introduced by Michel (1969) and the dimensionless power of the flow \hat{L} . In the case of the Crab, it was shown by LK that slow reconnection cannot dissipate the magnetic energy inside the radius at which observations imply that the wind terminates, independent of the value of μ . Faster dissipation prescriptions do not change this conclusion, provided standard estimates of the rate at which the pulsar injects pairs into the Nebula are adopted (Hibschman & Arons 2001a).

However, our calculations show that a higher injection rate permits faster dissipation. Thus, the σ -problem is resolved if dissipation is fast and $\mu \approx 2 \times 10^4$, corresponding to a pair flux of $\dot{N} = 3 \times 10^{40} \text{s}^{-1}$. This value is consistent with the model of the synchrotron spectrum of the Crab nebula presented by Gallant et al (2002). Lyubarsky & Eichler (2001) quote an even lower value of $\mu \approx 10^3$ from their considerations of the jet emerging from the Crab pulsar. In this case, the σ -problem is also resolved by dissipation proceeding at the tearing-mode limited rate. This suggests that most of the energy emitted by the Crab pulsar as

Poynting flux is converted into particle-born energy during the supersonic expansion phase of the wind. If a fraction of this power is converted into radiation, the dynamics of the flow imply that it will appear pulsed to an observer, which lends support to a recent suggestion concerning the origin of the optical to gamma-ray pulses from this object (Kirk et al 2002).

We thank Yves Gallant and Yuri Lyubarsky for stimulating discussions and helpful comments on this work.

A. The relativistic Harris equilibrium

The relativistic Vlasov equation:

$$\frac{\partial f}{\partial t} + \vec{v} \cdot \frac{\partial f}{\partial \vec{r}} + \dot{\vec{p}} \cdot \frac{\partial f}{\partial \vec{p}} = 0, \quad (\text{A1})$$

where \vec{v} is the particle 3-velocity, $\vec{p} = \gamma m \vec{v}$ the momentum (with $\gamma = 1/\sqrt{1 - v^2/c^2}$), f the Lorentz invariant phase-space density,

$$\dot{\vec{p}} = q \left(\vec{E} + \frac{1}{c} \vec{v} \wedge \vec{B} \right) \quad (\text{A2})$$

the Lorentz force, q the particle charge and \vec{E} and \vec{B} the electric and magnetic fields, is solved by an arbitrary function of the constants of motion.

In the case of a current sheet in the y - z plane, where quantities in (A1) depend on space only via x , the constants of motion are the energy and the y and z components of the canonical momentum:

$$\begin{aligned} E &= (m^2 c^4 + c^2 p^2)^{1/2}, \\ P_y &= p_y + \frac{q}{c} A_y(x), \\ P_z &= p_z + \frac{q}{c} A_z(x), \end{aligned} \quad (\text{A3})$$

where \vec{A} is the vector potential. We seek a solution in which the z component of \vec{B} reverses at $x = 0$. Choosing $A_z = 0$, this means $B_z = \partial A_y / \partial x = 0$ at $x = 0$. To this we can add a constant component along y by specifying $A_x = z B_y$, without affecting the following analysis.

Harris (1962) found a solution to this problem with a phase-space density which, at $x = 0$, consists of two Maxwellians, one for each species, drifting in opposite directions along

the y axis with zero charge density. The relativistic generalisation found by Hoh (1968) has two drifting Jüttner/Synge distributions. In the case with just positrons $q = e$ and electrons $q = -e$, these distributions drift with equal and opposite speeds $c\beta q/e$ and have equal and opposite charge densities. In terms of quantities measured in the rest frame of a species (denoted with a bar), the phase-space density of that component at $x = 0$ is

$$\bar{f}_{0\pm} = f_{0\pm} = \frac{\bar{N}}{4\pi m^2 c \Theta K_2(mc^2/\Theta)} \exp(-\bar{E}/\Theta), \quad (\text{A4})$$

where \bar{E} is the particle energy in the rest frame, Θ the temperature and K_2 a modified Bessel function. The distribution is normalized such that the particle number density is \bar{N} : $\int d^3p f = \bar{N}$.

Employing the Lorentz transformation

$$\bar{E} = \Gamma(E \mp c\beta p_y), \quad (\text{A5})$$

where the upper sign refers to the positrons, we can write the phase-space density at $x = 0$ in terms of lab. frame quantities:

$$f_{0\pm} = \frac{\bar{N}}{4\pi m^2 c \Theta K_2(mc^2/\Theta)} \exp\left[-\frac{\Gamma(E \mp c\beta p_y)}{\Theta}\right]. \quad (\text{A6})$$

Choosing $A_y(0) = 0$, the solution of the Vlasov equation which matches (A6) at $x = 0$ is

$$\begin{aligned} f_{\pm} &= \frac{\bar{N}}{4\pi m^2 c \Theta K_2(mc^2/\Theta)} \times \\ &\quad \exp\left[-\frac{\Gamma(E \mp c\beta p_y \mp q\beta A_y(x))}{\Theta}\right], \\ &= f_{0\pm} \exp\left[\frac{e\beta\Gamma A_y(x)}{\Theta}\right]. \end{aligned} \quad (\text{A7})$$

The current density carried by the electrons and positrons is:

$$j_y = \exp\left[\frac{e\beta\Gamma A_y(x)}{\Theta}\right] ec^2 \int d^3p \frac{p_y}{E} (f_{0+} - f_{0-}). \quad (\text{A8})$$

Using the invariance of d^3p/E :

$$\begin{aligned} \int d^3p \frac{p_y c^2}{E} f_{0\pm} &= \int d^3\bar{p} \frac{\bar{p}_y c^2}{\bar{E}} f_{0\pm}, \\ &= \int d^3\bar{p} \frac{c^2}{\bar{E}} \Gamma(\bar{p}_y \pm \beta\bar{E}/c) f_{0\pm}, \\ &= \pm \int d^3\bar{p} \Gamma\beta c f_{0\pm} = \pm\Gamma\beta c\bar{N}, \end{aligned} \quad (\text{A9})$$

so that

$$j_y = 2e\Gamma\beta c\bar{N}\exp\left[\frac{e\beta\Gamma A_y(x)}{\Theta}\right]. \quad (\text{A10})$$

Using the Maxwell equation $4\pi j_y/c = -\partial B_z/\partial x$ we find:

$$\frac{\partial^2 A_y}{\partial x^2} = -8\pi\beta e N'_\pm \exp\left[\frac{e\beta\Gamma A_y}{\Theta}\right], \quad (\text{A11})$$

where $N'_\pm = \Gamma\bar{N}$ is the number density of each species in the lab. frame.

With the boundary conditions $\partial A_y/\partial x = A_y = 0$ at $x = 0$ the solution of (A11) is

$$A_y = \frac{\Theta}{e\beta\Gamma} \ln [\text{sech}^2(x/a)],$$

with

$$(\text{A12})$$

$$a = \lambda_D/\beta,$$

$$\lambda_D = \sqrt{\frac{\Theta}{4\pi N'_\pm e^2\Gamma}}. \quad (\text{A13})$$

This is precisely the solution found by Harris (1962), with the substitution $T = \Theta/\Gamma$. The distribution function is

$$f_\pm = f_{0\pm}\text{sech}^2(x/a) \quad (\text{A14})$$

and the density and magnetic field are

$$n'_\pm = N'_\pm \text{sech}^2(x/a),$$

$$B' = \sqrt{\frac{16\pi N'_\pm \Theta}{\Gamma}} \tanh(x/a). \quad (\text{A15})$$

The number of particles per unit area of the sheet is

$$N'_{\text{tot}} = 2 \int_{-\infty}^{\infty} dx n'_\pm(x) = 4aN'_\pm. \quad (\text{A16})$$

To calculate the elements of the stress-energy tensor

$$T^{a,b} = \int \frac{d^3p}{E} p^a p^b (f_+ + f_-), \quad (\text{A17})$$

where $p^a = (E, cp)$ is the momentum 4-vector, it is convenient to transform to the rest frame of each species in turn and use the integrals

$$\begin{aligned} \int d^3\bar{p}\bar{E}f_{0\pm} &= \bar{N} \left[3\Theta + mc^2 \frac{K_1(mc^2/\Theta)}{K_2(mc^2/\Theta)} \right], \\ &\equiv \bar{N}R(mc^2/\Theta), \end{aligned} \quad (\text{A18})$$

$$\int d^3\bar{p}\frac{c^2\bar{p}^2}{\bar{E}}f_{0\pm} = 3\bar{N}\Theta, \quad (\text{A19})$$

to find:

$$T^{0,0} = 2n'_\pm \left[\Gamma(R + \Theta) - \frac{\Theta}{\Gamma} \right], \quad (\text{A20})$$

$$T^{1,1} = T^{3,3} = 2n'_\pm \frac{\Theta}{\Gamma}, \quad (\text{A21})$$

$$T^{2,2} = 2n'_\pm \left[\Gamma(R + \Theta) - \frac{R}{\Gamma} \right] \quad (\text{A22})$$

and all remaining elements zero. In the pulsar wind, purely radial motion is considered, with the sheet normal along the radius vector. In this case, only the $T^{0,0}$ and $T^{1,1}$ components are relevant and we can identify the effective enthalpy density and pressure: $w = 2n'_\pm\Gamma(R + \Theta)$, $p = 2n'_\pm\Theta/\Gamma$. This leads to an effective ratio of specific heats [see Lyubarsky & Kirk (2001) Eq. (A9)]:

$$\hat{\gamma} = 1 + \frac{\Theta}{\Gamma(\Gamma R - mc^2) + \Gamma^2\beta^2\Theta}. \quad (\text{A23})$$

B. The entropy condition Eq. (27)

Details of the derivation of eqs. (1), (2) and (3) are given in LK. Using the same notation, we derive here the condition that the specific entropy of a fluid element always increase, Eq. (27).

The fast phase variable ϕ and slow radius variable R , Eq. (A15) of LK are defined by

$$\begin{aligned} \phi &= \Omega \left[t - \int_{r_0}^r \frac{dr'}{v(r')} \right], \\ R &= \varepsilon r/r_L, \end{aligned} \quad (\text{B1})$$

where r_0 is an arbitrary point in the flow. The starting point of the derivation is the entropy equation written in terms of the energy density e' and entropy density w' in the co-moving

frame, this reads:

$$\begin{aligned} & \gamma \left(1 - \frac{v}{v_w} \right) \frac{\partial e'}{\partial \phi} + w' \left[\frac{\partial \gamma}{\partial \phi} - \frac{1}{R^2 v_w} \frac{\partial}{\partial \phi} (\gamma v R^2) \right] \\ & + \varepsilon \gamma v \frac{\partial e'}{\partial R} + \frac{\varepsilon w'}{R^2} \frac{\partial}{\partial R} (\gamma v R^2) = \frac{1}{\Omega} \gamma \left(E - \frac{v}{c} B \right) j \quad . \end{aligned} \quad (\text{B2})$$

Expanding the dependent variables as in Eq. (A18) of LK and collecting terms of zeroth order one finds, using conditions (A19–A22) of LK, that this equation is trivially satisfied, because the ohmic dissipative term $j' \cdot E'$ vanishes to zeroth order. To first order, we find an expression equivalent to (A27) of LK:

$$\begin{aligned} & -\frac{\gamma_0 v_1}{v_0} \frac{\partial e'_0}{\partial \phi} - \frac{\gamma_0 w'_0}{v_0} \frac{\partial v_1}{\partial \phi} + \gamma_0 v_0 \frac{\partial e'_0}{\partial R} + \frac{w'_0}{R^2} \frac{\partial}{\partial R} (\gamma_0 v_0 R^2) \\ & = \frac{\gamma_0 v_1}{v_0} \frac{\partial p_0}{\partial \phi} - \frac{B_0}{4\pi \gamma_0 R} \frac{\partial}{\partial R} (R v_0 B_0) \quad , \end{aligned} \quad (\text{B3})$$

in which the right hand-side is proportional to the ohmic dissipation. To derive the entropy equation Eq. (3), this equation is integrated over ϕ and exact periodicity is imposed upon the expanded dependent variables. However, in order to obtain Eq. (27), we instead impose the restriction that the ohmic dissipation be positive:

$$\begin{aligned} & -\frac{\gamma_0 v_1}{v_0} \frac{\partial e'_0}{\partial \phi} - \frac{\gamma_0 w'_0}{v_0} \frac{\partial v_1}{\partial \phi} \\ & + \gamma_0 v_0 \frac{\partial e'_0}{\partial R} + \frac{w'_0}{R^2} \frac{\partial}{\partial R} (\gamma_0 v_0 R^2) > 0 \quad . \end{aligned} \quad (\text{B4})$$

In order to integrate this condition, we introduce the ratio of specific heats $\hat{\gamma}$ as in Eq. (12) and assume this to be constant. Multiplying by the (positive) factor $p'^{-(\hat{\gamma}-1)/\hat{\gamma}}$, integrating and imposing exact periodicity leads to:

$$\left\langle \frac{\partial}{\partial R} \left(R^2 \gamma_0 v_0 p_0^{1/\hat{\gamma}} \right) \right\rangle > 0 \quad . \quad (\text{B5})$$

Noting that for the Harris current sheet

$$\left\langle p_0^{1/\hat{\gamma}} \right\rangle = \left(\frac{B_0'^2}{8\pi} \right)^{1/\hat{\gamma}} \Delta \left\{ \frac{1}{2} \int_{-\infty}^{\infty} dx [\text{sech}(x)]^{2/\hat{\gamma}} \right\} \quad , \quad (\text{B6})$$

we arrive, after introducing the dimensionless variables used in Sect. 3, at condition (27).

C. Expansion speed of the current sheet

Assuming the sheet is bounded in the comoving frame by a forward and a backward moving front at $r = r_+(r, t)$ and $r_-(r, t)$, respectively, we can write their speeds in the lab. frame as

$$\frac{dr_{\pm}}{dt} = \frac{v \pm c\beta_c}{1 \pm v\beta_c/c}, \quad (\text{C1})$$

where $\pm\beta_c$ are the speeds of the fronts measured in an inertial frame moving with the speed of the wind at (r, t) . In terms of the fast phase and slow radius variables, Eq. (B1), we find

$$\frac{d\phi_{\pm}}{dR} = \frac{-(dr_{\pm}/dt)(\partial t/\partial R) + (\partial r/\partial R)}{-(dr_{\pm}/dt)(\partial t/\partial\phi) + (\partial r/\partial\phi)}. \quad (\text{C2})$$

The fraction of one wavelength occupied by the two sheets thus evolves according to

$$\begin{aligned} \frac{d\Delta}{dR} &= \frac{1}{\pi} \frac{d}{dR} (\phi_+ - \phi_-), \\ &= \frac{2\beta_c c^2}{\pi \varepsilon \gamma^2 (v^2 - c^2 \beta_c^2)}. \end{aligned} \quad (\text{C3})$$

This is equivalent to Eq. (31), provided r is identified as a ‘slow’ variable.

REFERENCES

- Arons J., 1983 in *Electron-Positron Pairs in Astrophysics* Eds. M.L. Burns, A.K. Harding, R. Ramaty (New York: American Institute of Physics), p. 163
- Begelman, M.C., Li Z.-Y., 1992 ApJ 397, 187
- Beskin V.S., Kuznetsova I.V., Rafikov R.R., 1998 MNRAS 299, 341
- Biskamp D., 2000 “Magnetic reconnection in plasmas” (Cambridge University Press, Cambridge)
- Bogovalov S.V., 1999 A&A 349, 1017
- Bogovalov S.V., 2001 A&A 371, 1155
- Bogovalov S.V., Tsinganos K. 1999 MNRAS 305, 211
- Büchner J., Kuska J.P. 1999 Ann. Geophys. 17, 604

- Buckley R. 1977 MNRAS 180, 125
- Chiueh T., Li Z.Y., Begelman M.C. 1998 ApJ 505, 835
- Coroniti F.V. 1990 ApJ 349, 538
- Daughton W. 1999 Phys. Plasmas 6, 1329
- Drenkhahn G. 2002 A&A 387, 714
- Drenkhahn G., Spruit H.C. 2002 A&A 391, 1141
- Emmering R.T., Chevalier R.A. 1987 ApJ 321, 334
- Gallant Y.A., van der Swaluw E., Kirk J.G., Achterberg A. 2002 in “Neutron Stars in Supernova Remnants”, Eds: P.O. Slane, B.M. Gaensler, ASP Conference Series Vol. 271, 99
- Gunn J.E., Ostriker J.P., 1969 Nature 221, 454
- Harris E.G. 1962 Nuovo Cimento 23, 115
- Heinz S., Begelman M.C. 2000 ApJ 535, 104
- Hesse M., Kuznetsova M., Birn J. 2001 J. Geophys. Res. Space Phys. 106, 29831
- Hirschman J.A., Arons J. 2001a ApJ 554, 624
- Hirschman J.A., Arons J. 2001b ApJ 560, 871
- Hoh F.C. 1968 Physics Fluids 9, 277
- Contopoulos I., Kazanas D. 2002 ApJ 566, 336
- Kennel C.F., Coroniti F.V., 1984 ApJ 283, 694
- Kirk J.G., Duffy P. 1999 J. Phys. G: Nucl. Part. Phys. 25, R163
- Kirk J.G., Skjæraasen O., Gallant Y.A. 2002 A&A 388, L29
- Kuijpers J. 2001 Publ Astron. Soc. Aust. 18, 407
- Lovelace R.V.E., Li H., Koldoba A.V., Ustyugova G.V., Romanova, M.M. 2002 ApJ 572, 445
- Lyubarsky Y. 1996 A&A 311, 172

- Lyubarsky Y. 2002a MN 329, L34
- Lyubarsky Y. 2002b MN in press, astro-ph/0211046
- Lyubarsky Y., Eichler D. 2001 ApJ 562, 494
- Lyubarsky Y., Kirk J.G. 2001 ApJ 547, 437 (LK in text)
- Lyutikov M., Blackman E.G. 2001 MN, 321, 177
- Lyutikov M., Uzdensky D. 2002 astro-ph/0210206
- Melatos A. 2002 in ‘Neutron Stars and Supernova Remnants’ ASP Conf. Series Vol. 271, Eds: P.O. Slane and B.M. Gaensler, ASP, San Francisco, page 115
- Melatos A., Melrose D.B. 1996 MN 279, 1168
- Melrose D.B. 1986 “Instabilities in space and laboratory plasmas”, Cambridge University Press, Cambridge
- Michel, F.C., 1969 ApJ 158, 727
- Michel, F.C., 1982 Rev. Mod. Phys. 54, 1
- Michel, F.C., 1994 ApJ 431, 397
- Priest E.R., Forbes T. 2000 “Magnetic Reconnection” (Cambridge University Press, Cambridge)
- Pritchett P.L., Coroniti F.V., Decyk V.K. 1996 J. Geophys. Res. Space Phys. 101, 27413
- Rees M.J., Gunn J.E., 1974 MNRAS 167, 1
- Schopper R., Lesch H., Birk G.T. 1998 A&A 335, 26
- Skjæraasen O., Kirk J.G. 2001 in “Similarities and universality in relativistic flows” Eds: Georganopoulos, Guthmann, Manolakou, Marcowith (Logos Verlag, Berlin)
- Skjæraasen O., Kirk J.G., Y.A. Gallant 2002 in ‘Neutron Stars and Supernova Remnants’ ASP Conf. Series Vol. 271, Eds: P.O. Slane and B.M. Gaensler, ASP, San Francisco, page 87
- Somov B.V., Titov V.S. 1985 Solar Physics 102, 79
- Spruit H.C. 1999 A&A 341, L1

- Spruit H.C., Daigne, F., Drenkhahn G. 2001 A&A 369, 694
- Thompson C. 1994 MN 270, 480
- Usov V.V., 1975 Astrophys. & Space Sci. 32, 375
- Usov V.V., 1992 Nature 357, 472
- Weisskopf M., Hester J.J., Tennant A.F., Elsner R.F., Schulz N.S., Marshall H.L., Karovska M., Nichols J.S., Swartz D.A., Kolodziejczak J.J., O'Dell S.L. 2000 ApJ 536, L81
- Zelenyi L.M., Krasnosel'skikh V.V. 1979 Sov. Phys. A.J. 56, 819
- Zenitani S., Hoshino M. 2001 ApJ 562, L63
- Zhu Z.W., Winglee R.M. 1996 J. Geophys. Res. Space Phys. 101, 4885

Table 1. Asymptotic flow properties for different dissipation prescriptions. Given are the index q in Eqs. (40–41), the approximate radius r_{\max} at which dissipation is complete, the approximate radius r_{\min} at which the solution crosses the fast magnetosonic point and the exact (asymptotic) expression for Δ . The light-cylinder radius is denoted by r_{L} , Δ is the thickness in units of the pattern half-wavelength, μ is the total energy carried by the wind per unit rest mass ($\times c^2$), \hat{L} is the dimensionless flow luminosity defined in Eq. (29), and β_c is the sheet expansion speed in the comoving frame, in units of c .

	q	r_{\max}/r_{L}	r_{\min}/r_{L}	$\Delta (r/r_{\text{L}})^{-q}$
Slow dissipation (Eq. 30)	1/2	$\hat{L}^{1/2}$	$\mu^{-4/3} \hat{L}^{1/2}$	$\frac{1}{\sqrt{6}} \hat{L}^{-1/4}$
Tearing mode limited dissipation (Eq. 37)	5/12	$\mu^{4/5} \hat{L}^{3/10}$	$\mu^{-4/5} \hat{L}^{3/10}$	$\left(\frac{5^8}{19^7 12 \pi^2}\right)^{1/12} \mu^{-1/3} \hat{L}^{-1/8}$
Fast dissipation (Eqs. 31 & 33)	1/3	$0.1 \mu^2 (1 - \beta_c^2) / \beta_c$	$0.1 (1 - \beta_c^2) / \beta_c$	$\left(\frac{6 \beta_c}{25 \pi (1 - \beta_c^2)}\right)^{1/3} \mu^{-2/3}$